Substrate Specificity of Sugar Transport by Rabbit SGLT1: Single-Molecule Atomic Force Microscopy versus Transport Studies†

Theeraporn Puntheeranurak,[‡,§,||] Barbara Wimmer,[§,||] Francisco Castaneda,[§] Hermann J. Gruber,[||] Peter Hinterdorfer,[||] and Rolf K. H. Kinne*[,§]

Department of Biology and Center of Nanoscience and Nanotechnology, Faculty of Science, Mahidol University, Bangkok 10400, Thailand, Department of Epithelial Cell Physiology, Max Planck Institute of Molecular Physiology, Otto-Hahn-Strasse 11, Dortmund 44227, Germany, and Institute for Biophysics, Johannes Kepler University of Linz, Altenbergerstrasse 69, Linz A-4040, Austria

Received September 15, 2006; Revised Manuscript Received December 18, 2006

ABSTRACT: In the apical membrane of epithelial cells from the small intestine and the kidney, the high-affinity Na^+/D-glucose cotransporter SGLT1 plays a crucial role in selective sugar absorption and reabsorption. How sugars are selected at the molecular level is, however, poorly understood. Here atomic force microscopy (AFM) was employed to investigate the substrate specificity of rbSGLT1 on the single-molecule level, while competitive-uptake assays with isotope-labeled sugars were performed in the study of the stereospecificity of the overall transport. *rbSGLT1*-transfected Chinese hamster ovary (CHO) cells were used for both approaches. Evidence of binding of D-glucose to the extracellular surface of rbSGLT1 could be obtained using AFM tips carrying 1-thio-D-glucose coupled at the C1 position to a PEG linker via a vinylsulfon group. Competition experiments with monosaccharides in solution revealed the following selectivity ranking of binding: 2-deoxy-D-glucose ≥ 6-deoxy-D-glucose > D-glucose > D-galactose ≥ α-methyl glucoside; 3-deoxy-D-glucose, D-xylose, and L-glucose did not measurably affect binding. These results were different from those of competitive α-methyl glucoside transport assays, where the ranking of inhibition was as follows: D-glucose > D-galactose > 6-deoxy-D-glucose; no uptake inhibition by D-xylose, 3-deoxy-D-glucose, 2-deoxy-D-glucose, or L-glucose was observed. Taken together, these results suggest that the substrate specificity of SGLT1 is determined by different recognition sites: one possibly located at the surface of the transporter and others located close to or within the translocation pathway.

Secondary active transport is a fundamental biological principle (*1*, *2*). Na^+/D-glucose cotransporter type 1 (SGLT1) is one of the most intensively studied membrane transporters (*3*, *4*). SGLT1 is a member of a very large solute carrier family (SLC5) which transports various solutes into cells using the Na^+ electrochemical potential gradient across the plasma membrane (*5*). Intestinal glucose absorption and renal glucose reabsorption in many species are Na^+-dependent and crucially mediated by SGLT1 (*1*). Rabbit SGLT1 was first cloned by Hediger and colleagues in 1987 (*6*) and since then has been studied extensively. A defect in SGLT1 can cause glucose-galactose malabsorption (GGM) which is an autosomal recessive disease (*7*). Recently, strong interest has been focused on inhibitors of the novel target SGLT (SGLT1 and SGLT2) for potential therapy of type 2 diabetes (*8*, *9*).

It has been proposed that SGLT1 contains 14 transmembrane α-helices with both the N- and C-termini facing the extracellular compartment (*10*−*12*). With regard to the structure−function relationship, the N-terminal half of SGLT1 participates in Na^+ binding while the C-terminal domain, particularly helices 10−13 of the protein, participates in sugar transport (*13*−*16*). Cotransport is supposed to be initiated when two external Na^+ ions bind to the SGLT1 and induce structural alterations in the protein, which allow sugar binding, followed by the simultaneous translocation of sodium and sugar across the membrane (*3*). From transport studies in intact cells and brush border membrane vesicles, it is known that SGLT1 strongly discriminates among monosaccharides, D-glucose and D-galactose being the natural substrates (*17*−*20*). Although these former studies outlined the important structural and conformational features required for a sugar to be transported, the question of how the transporter SGLT1 selects its substrates was not investigated.

In previous studies, we have demonstrated that atomic force microscopy (AFM;[1] see ref *21*) is a powerful approach to studying the presence and dynamics of membrane transporters in intact cells on the single-molecule level (*22*). The high sensitivity of AFM and the soft cantilever that is

† This work was supported in part by the Thailand Research Fund and the Commission on Higher Education (T.P.), Austrian Science Foundation Project P-14549 (P.H.), and the Max Planck Institute for Molecular Physiology.

* To whom correspondence should be addressed: Max Planck Institute of Molecular Physiology, Otto-Hahn-Str. 11, Dortmund 44227, Germany. E-mail: rolf.kinne@mpi-dortmund.mpg.de. Telephone: +49 (0) 231-133-2220. Fax: +49 (0) 231-133-2699.

‡ Mahidol University.

§ Max Planck Institute of Molecular Physiology.

|| Johannes Kepler University of Linz.

[1] Abbreviations: rbSGLT1, sodium/D-glucose cotransporter 1 (rabbit isoform); AFM, atomic force microscopy; CHO, Chinese hamster ovary; AMG, α-methyl glucoside; PEG, poly(ethylene glycol); VS, vinylsulfonylbenzyl group; SH, sulfhydryl; NHS, *N*-hydroxysuccinimide.

10.1021/bi061917z CCC: $37.00
Published on Web 02/16/2007

used offer the potential to detect picoNewton forces of transporter−ligand complexes, which provides a unique opportunity to detect molecular recognition of binding events under different environmental conditions (*23*−*26*).

Here we investigate the initial molecular recognition of D-glucose with SGLT1 on the cell membrane surfaces of living cells by using D-glucose coupled at the C1 position to AFM tips. The results obtained in this study reveal that the stereospecificity of the initial binding of D-glucose to SGLT1 generated from AFM force spectroscopy differs from that obtained under identical conditions in competitive transport assays in which isotope-labeled α-methyl glucoside ([^{14}C]AMG) was taken up by cells. These data support the hypothesis that at least two sites of interaction of the transporter with the sugars where selection occurs exist, one feasibly involved in the initial binding step and the other in the translocation reaction.

EXPERIMENTAL PROCEDURES

Materials. 1-thio-β-D-glucose, β-D-glucose, L-glucose, D-galactose, D-xylose, 2-deoxy-D-glucose, 3-deoxy-D-glucose, 6-deoxy-D-glucose, α-methyl glucoside, phlorizin, and poly-L-lysine were purchased from Sigma (Schnelldorf, Germany). All other reagents were of the highest available purity.

Cell Cultures. rbSGLT1-expressing G6D3 cells, a CHO cell line stably transfected with rabbit SGLT1 generated in our laboratory (*27*), were grown in 25 cm^2 flasks (Falcon, Heidelberg, Germany) under 5% CO_2 at 37 °C. This cell line was cultured in Dulbecco's modified Eagle's medium (DMEM), containing high glucose (25 mM) supplemented with 5% fetal calf serum, 1 mM sodium pyruvate, 2 mM L-glutamine, 1× minimal essential medium, and 25 μM β-mercaptoethanol. Culture medium contained 400 μg/mL paneticin G420 (PAN Biotech GmbH, Aidenbach, Germany) to maintain selection of transfected cells. Culture medium was renewed three times per week, and the cells were subcultured at 80% confluence. Cell passages below 15 were used for all experiments. For AFM studies, the cells were seeded on 22 mm^2 poly-L-lysine-coated glass cover slips and the experiments were performed within 1−4 days of seeding. For uptake studies, confluent monolayers of G6D3 cells were grown on 96-well plates (Falcon) for 3 days.

Transport Studies. Na^+/D-glucose cotransport activity and phlorizin inhibition were assessed by examining α-[^{14}C]AMG (specific radioactivity of 300 mCi/mmol) uptake as described previously (*28*). A 96-well automated method was employed so that small amounts of the radioactive compound and inhibitory substances could be used. Briefly, the cells were incubated in a D-glucose-free medium for 1 h at 37 °C prior the transport assays. For the purpose of this study, Krebs-Ringer-HEPES (KRH) solution containing 120 mM NaCl, 4.7 mM KCl, 2.2 mM $CaCl_2$, 1.2 mM $MgCl_2$, and 10 mM HEPES (pH 7.4 with Tris base) was used to asses sodium-dependent D-glucose transport. Cytochalasin B (50 μM) was added as a supplement to KRH solution to suppress glucose uptake by GLUT protein (glucose transporter). A KRH solution containing 120 mM *N*-methylglucamine (NMG) instead of NaCl was used to assess sodium-independent D-glucose transport. The uptake activity assay with the three transport buffers containing KRH-Na^+ or KRH-Na^+ with phlorizin (0.5 mM) or KRH-NMG with 0.1 mM AMG (containing 1 μCi/mL ^{14}C-labeled AMG) was performed by using a MicroBeta Trilux (Perkin-Elmer). Then luminescence ATP detection was assessed to determine the amount of protein, and the mean counts per minute (cpm) were calculated. The results were expressed as cpm (mg/mL protein)$^{-1}$ (30 s)$^{-1}$ as mean values ± the standard error of the mean ($n = 3$). The statistical significance was tested using a Student's *t*-test.

Competition Assays. The competitive measurements of AMG uptake were performed in the presence of several competitive sugars, i.e., D-glucose, L-glucose, D-galactose, D-xylose, 2-deoxy-D-glucose, 3-deoxy-D-glucsoe, and 6-deoxy-D-glucose at concentrations of 0.5, 5, and 10 mM. Transport buffer containing a KRH-Na^+ solution, 50 μM cytochalasin B, and 0.1 mM AMG (containing 1 μCi/mL ^{14}C-labeled AMG) was used throughout these inhibition studies. The results were expressed as cpm (mg/mL protein)$^{-1}$ (30 s)$^{-1}$ as mean values ± the standard error of the mean ($n = 3$). The value of AMG uptake in the absence of the competitive sugars was employed for calculation of a percent reduction for each inhibition.

Conjugation of 1-Thioglucose to AFM Tips. Conjugation of 1-thio-β-D-glucose to AFM tips via a flexible PEG [poly(ethylene glycol)] cross-linker was carried out as described previously (*22*). In brief, silicon tips were first functionalized with ethanolamine by an overnight incubation with ethanolamine hydrochloride solubilized in DMSO. In the second step, the NHS (*N*-hydroxysuccinimide) ester function of the PEG linker (VS-PEG-NHS) was covalently bound to amino groups on the tip surface. In the third step, the free SH group of 1-thio-β-D-glucose was reacted with VS (vinylsulfon)-PEG-conjugated AFM tips. Tips were finally washed in the AFM working buffer and stored in the cold room. This method provides tips which are suitable for single-molecule recognition studies.

Atomic Force Microscopy and Spectroscopy. All AFM investigations were performed using a magnetically driven dynamic force microscope (PicoSPM II, Molecular Imaging, Tempe, AZ) in the Na^+-containing KRH medium except where Na^+-free medium was stated. For the detection of glucose−SGLT1 recognition, force−distance cycles were performed at room temperature using glucose-coated cantilevers (rectangular cantilever, Veeco Instruments, Mannheim, Germany) with a nominal spring constant of 0.02 N/m in the conventional contact force spectroscopy mode as described previously (*22*). Force−distance cycles were recorded on cell surfaces with the assistance of a CCD camera for positioning the AFM cantilever on isolated cells or cell monolayers (living cells). The sweep amplitude of the force−distance cycles was 1000 nm at a sweep rate of 1 Hz. Up to 500−1000 force−distance cycles were performed for each location on the surface of cells and up to four locations (different cells) for each condition, i.e., initial condition, ligand addition, and washout condition. For ligand addition, D-glucose, L-glucose, D-galactose, D-xylose, 2-deoxy-D-glucose, 3-deoxy-D-glucsoe, 6-deoxy-D-glucose, AMG (10 mM each) or 0.5 mM phlorizin was separately applied for competitive investigations. Force−distance cycles were recorded after incubation with the ligand for 10 min. The washing periods were ∼30 min to 1 h to ensure complete removal of ligand. The binding probability for each condition was derived and expressed as the mean value ± the standard

error of the mean ($n = 2000-4000$). The statistical significance was tested using a Student's *t*-test. Several experiments were performed, and one typical experiment for each condition is shown.

For the quantification of the forces, spring constants of cantilevers were determined in air using the thermal noise method (*29*, *30*). The deflection sensitivity of the photodetector was determined from the slope of the force−distance curves taken on the bare surface of glass cover slips. Analysis of interaction forces was performed using Matlab version 6.5 (Math Works, Natick, MA) as previously described (*23*, *31*).

RESULTS

Interaction of Sugars with rbSGLT1 As Observed by AFM Force Spectroscopy. AFM force spectroscopy was employed in investigating sugar−SGLT1 interactions at the single-molecule level. An AFM tip sensor was designed in which the OH groups known to be essential for translocation (i.e., at C2, C3, and C4) were not modified (*18*, *32*−*39*), and the ligand was tightly attached to the tip. The AFM tips were covalently conjugated with 1-thio-β-D-glucose via a distensable linker (VS-PEG-NHS; see Experimental Procedures) at a very dilute surface density. The construction of the ligand−AFM tip creating the 1-thio-D-glucose tip is depicted in Figure 1A. The NHS ester function of the PEG linker was covalently attached to amino groups on the modified tip surface. Then the free thiol group at the C1 position of 1-thio-β-D-glucose was coupled to the VS end forming a thio−glycosidic bond.

The principle of single-molecule recognition force detection of the ligand−receptor complex on living G6D3 cells by using AFM is illustrated in Figure 1B. In this so-called force−distance mode, the deflection angle of the cantilever is measured as a function of the vertical position of the cantilever.

A single-molecule recognition event of D-glucose with SGLT1 on the surface of a G6D3 cell with the thioglucose-conjugated tip is shown as a typical force curve (retraction) in Figure 2. Considering the size of the bulky *p*-vinylsulfonylbenzyl group (*40*), this interaction very probably represents an initial binding of the glucose to SGLT1 which is not followed by translocation. Distinct recognition events were only observed in the presence of sodium (Figure 2), and no binding events were observed in sodium-free buffer when sodium was replaced with *N*-methyl-D-glucamine (inset of Figure 2). The observed probabilities of binding (probability of finding an unbinding event in force−distance cycles) of D-glucose to SGLT1 ranged from 8 to 12%, binding events being detected only in CHO cells overexpressing rbSGLT1 (data not shown). Furthermore, the interactions were inhibited by phlorizin (see below), a competitive specific inhibitor of SGLT. These data establish that the binding events occur at the surface of SGLT1 molecules. By constructing an empirical probability density function of the unbinding force, we found the maximum of the distribution function to be ~40−50 pN [for more detail, see previous studies (*22*)].

Stereospecificity of the Initial D-Glucose-Binding Site. The effect of various sugars, including some controvertible sugars, on the probability of binding of the 1-thio-D-glucose tip to the transporter with the block-washout experiments is shown in Figure 3. In the absence of sugar, the probabilities of binding of the tip to SGLT1 in KRH-Na^+ buffer were similar (Figure 3A−H, first bar). These values were in agreement with the ones from the previous studies (*22*). Upon injection of 10 mM free sugars into the medium, the binding

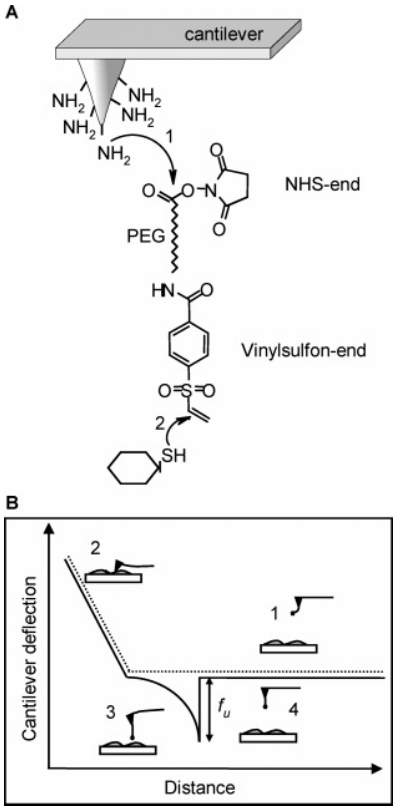

FIGURE 1: Single-molecule recognition using AFM force spectroscopy. (A) Linkage of glucose to AFM tips. 1-thio-glucose was covalently coupled to AFM tips via a heterobifunctional PEG derivative (VS-PEG-NHS) 8 nm in length. The NHS end of the PEG linker was covalently bound to amines on the functionalized tip surface (1), and glucose was attached to the VS end via a free thiol (2). (B) Schematic representation of a force−distance cycle carried out to measure specific molecular force. The tip was moved toward the cell surface (dotted line, 1−2) and then retracted (solid line) at a constant lateral position. During tip approach, the ligand specifically binds with a receptor that leads to a force signal with a distinct shape (3) during tip retraction. The force increases until bond rupture occurs (4) at an unbinding force (f_u).

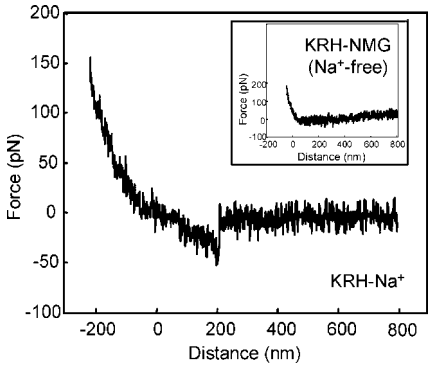

FIGURE 2: Force curve showing specific interaction between the glucose and SGLT1 upon tip−surface retraction. The retraction curve on the cell surface with a glucose-coated AFM tip shows a specific interaction in the presence of Na^+ (KRH-Na^+). The specific recognition disappears in the absence of Na^+ (KRH-NMG, inset).

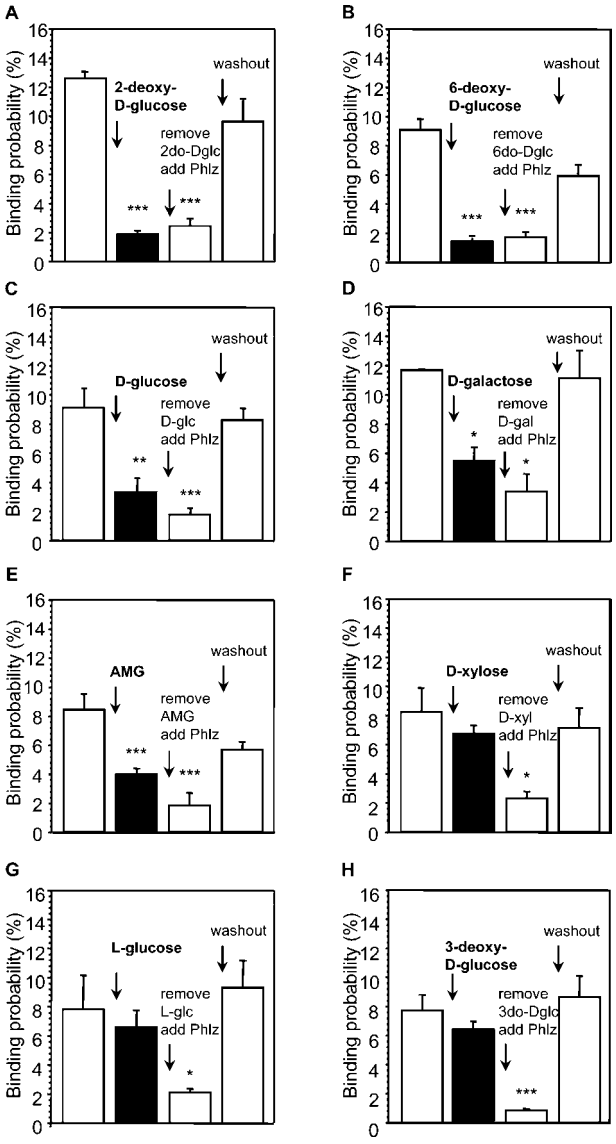

FIGURE 3: Inhibition of initial D-glucose binding. Binding probabilities of the D-glucose tip and effect of 2-deoxy-D-glucose (A, black bar), 6-deoxy-D-glucose (B, black bar), D-glucose (C, black bar), D-galactose (D, black bar), AMG (E, black bar), D-xylose (F, black bar), L-glucose (G, black bar), and 3-deoxy-D-glucose (H, black bar). Values are means ± the standard error of the mean (n = 2000−4000). Abbreviations: 2do-Dglc, 2-deoxy-D-glucose; 6do-Dglc, 6-deoxy-D-glucose; D-glc, D-glucose; D-gal, D-galactose; AMG, α-methyl glucoside; D-xyl, D-xylose; L-glc, L-glucose; 3do-Dglc, 3-deoxy-D-glucose; Phlz, phlorizin. $p < 0.05$ (one asterisk), $p < 0.01$ (two asterisks), and $p < 0.005$ (three asterisks) compared with levels in the relevant controls (absence of sugars or phlorizin in solution, value from the first bar).

probabilities were significantly reduced by 2-deoxy-D-glucose (from 12.6 ± 0.5 to 1.9 ± 0.3%, $p = 0.000003$), 6-deoxy-D-glucose (from 9.1 ± 0.8 to 1.5 ± 0.4%, $p = 0.0001$), D-glucose (from 9.3 ± 1.3 to 3.3 ± 0.9%, $p = 0.0086$), D-galactose (from 11.7 ± 0.1 to 5.5 ± 0.9%, $p = 0.0109$), and AMG (from 8.5 ± 1.1 to 4.0 ± 0.4%, $p = 0.0081$). Under the same experimental conditions, however, 3-deoxy-D-glucose (from 7.7 ± 1.1 to 6.4 ± 0.5%, $p = 0.3289$), D-xylose (from 8.3 ± 1.6 to 6.8 ± 0.5%, $p = 0.3657$), and L-glucose (from 7.8 ± 2.4 to 6.6 ± 1.2%, $p = 0.6576$) had no significant effect. These values are compiled as the percent inhibition of binding in Table 1. The ranking of the sugars with regard to the potency to prevent binding is as follows: 2-deoxy-D-glucose ≥ 6-deoxy-D-glucose > D-glucose > D-galactose ≥ AMG ≫ D-xylose ≥ 3-deoxy-D-glucose > L-glucose.

Table 1: Effect of Various Sugars on the Probability of Binding of D-Glucose to SGLT1 (AFM studies)

sugars and derivatives	% reduction[a]
2-deoxy-D-glucose	84.9
6-deoxy-D-glucose	83.5
D-glucose	64.5
D-galactose	53.0
α-methyl glucoside	52.9
D-xylose	18.0
3-deoxy-D-glucose	16.9
L-glucose	15.4

[a] The values were derived from the experiments depicted in Figure 3. In each experiment, 2000−4000 force−distance curves which were obtained at four different positions on the cell surface were analyzed.

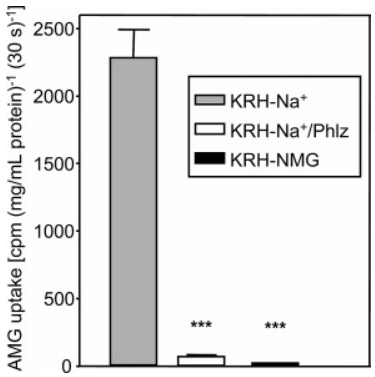

FIGURE 4: Representative experiment of uptake of [^{14}C]AMG by SGLT1 stably transfected G6D3 cells. Uptake was assessed by incubation with 0.1 mM AMG (containing 1 μCi/mL ^{14}C-labeled AMG) for 30 min at 37 °C under three conditions, i.e., in the presence of Na^+ (KRH-Na^+, gray bar), in the presence of Na^+ with specific inhibitor phlorizin (KRH-Na^+/Phlz, white bar), and in the absence of Na^+ (KRH-NMG, black bar). Values are means ± the standard error of the mean (n = 3); $p < 0.005$ (three asterisks) compared with levels in the presence of Na^+ (gray bar).

After free sugar was removed, phlorizin, a specific high-affinity competitive inhibitor which binds on the external membrane surface of SGLT1, was added to the solution. For 6-deoxy-D-glucose and 2-deoxy-D-glucose, the inhibition was comparable to that achieved with 0.5 mM phlorizin (Figure 3A,B).

Transport Studies in CHO Cells Overexpressing rbSGLT1 (G6D3 Cells). AMG uptake was performed to verify the functional activity of SGLT1 in the G6D3 cells. AMG is a substrate specific for SGLT1 and not transported by other sugar (sodium-independent) transport systems present in these cells. The results of transport studies using the 96-well automated method are shown in Figure 4. Na^+-dependent D-glucose cotransport assessed by [^{14}C]AMG uptake was 2284.4 ± 207.3 cpm (mg/mL protein)$^{-1}$ (30 s)$^{-1}$ (n = 3) in the presence of Na^+ (KRH-Na^+) and 20.9 ± 3.2 cpm (mg/mL protein)$^{-1}$ (30 s)$^{-1}$ (n = 3) in the absence of Na^+ (KRH-NMG). Phlorizin inhibition was confirmed by measuring the level of [^{14}C]AMG uptake in the presence of Na^+ and phlorizin, yielding 69.2 ± 14.7

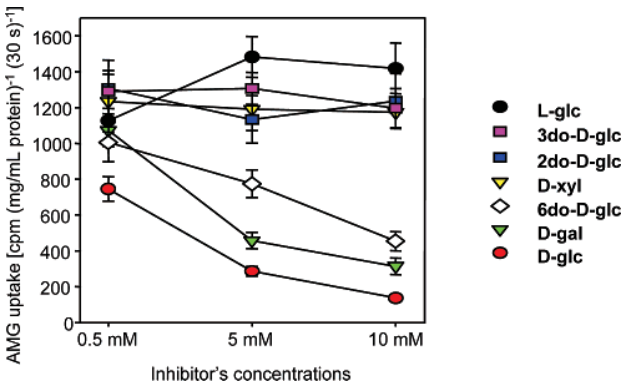

FIGURE 5: AMG uptake in the presence of competitive sugars. Uptake was assessed by incubation with 0.1 mM AMG (containing 1 μCi/mL ^{14}C-labeled AMG) together with each competitive sugar for 30 min at 37 °C in KRH-Na^+ medium. The levels of uptake at competitive sugar concentrations of 0.5, 5, and 10 mM, i.e., L-glucose (black circles), D-glucose (red circles), D-galactose (green triangles), D-xylose (yellow triangles), 2-deoxy-D-glucose (blue rectangles), 3-deoxy-D-glucsoe (pink rectangles), and 6-deoxy-D-glucose (white diamonds), were compared. Values are means ± the standard error of the mean ($n = 3$).

Table 2: Effect of Various Sugars on the Uptake of AMG by SGLT1 (transport studies)

sugars and derivatives	% reduction[a]
D-glucose	90.2
D-galactose	77.3
6-deoxy-D-glucose	67.2
D-xylose	15.1
3-deoxy-D-glucose	13.3
2-deoxy-D-glucose	10.5
L-glucose	−2.8

[a] The data were calculated by using the value of AMG uptake at 0.1 mM as a reference value.

cpm (mg/mL protein)$^{-1}$ (30 s)$^{-1}$ ($n = 3$). These data demonstrate that the expressed SGLT1 in this study shows the characteristic of Na^+ dependence and phlorizin sensitivity of transport.

Substrate Specificity of Transport. To investigate the substrate specificity exhibited in the more complex transport reaction of rbSGLT1, competitive uptake assays using isotope-labeled AMG were performed by adding various sugars to the uptake solutions. The levels of AMG uptake at concentrations of 0.5, 5, and 10 mM for competitive sugars, i.e., D-glucose, L-glucose, D-galactose, D-xylose, 2-deoxy-D-glucose, 3-deoxy-D-glucsoe, and 6-deoxy-D-glucose, are shown in Figure 5. In the absence of competing sugars, the level of AMG transport was 1380.4 ± 211.9 cpm (mg/mL protein)$^{-1}$ (30 s)$^{-1}$ ($n = 3$). Only D-glucose, D-galactose, and 6-deoxy-D-glucose inhibited AMG uptake in a dose-dependent manner, whereas the others sugars did not.

The percent reductions in the level of AMG uptake in the presence of each competitive sugar (10 mM) are compiled in Table 2. D-Glucose exhibited the strongest inhibition of AMG uptake (90.2%). The ranking of percent reduction from competitive assays (Table 2) was as follows: D-glucose > D-galactose > 6-deoxy-D-glucose ≫ D-xylose ∼ 3-deoxy-D-glucose ∼ 2-deoxy-D-glucose > L-glucose.

DISCUSSION

AFM Force Spectroscopy of the Interaction of D-Glucose with SGLT1. At present, atomic force microscopy is widely accepted as a tool in nano-bioscience and nano-biotechnology. The AFM approach is very useful in obtaining direct information either on isolated molecules or on the surface of living cells (for reviews, see refs *22* and *41*). It is noteworthy that our study was performed with unfixed cells under near-physiological conditions in terms of ion composition of the intra- and extracellular medium, membrane potential, and membrane fluidity.

For the detection of SGLT1 with D-glucose, we used interaction force spectroscopy. SGLT1-expressing G6D3 cells were firmly attached to poly-L-lysine-coated glass cover slips. This method of preparation is suitable for maintaining cell attachment and prolonging experimental time (*22*). To detect single-molecule events, single-molecule tips that contain a very low surface density of ligands (∼400 molecules/μm^2) were employed (*23*). At a given time, only one ligand has access to the transporters present at the cell surface. Here the AFM tips were covalently conjugated with 1-thio-β-D-glucose via distensable tethers which guarantees a sufficiently stable attachment, because these covalent bonds are ∼10 times stronger than typical ligand−receptor interactions (*41*). The NHS-PEG-VS cross-linker was purposely selected for this investigation since the bulky *p*-vinylsulfonylbenzoyl group present at the end of the linker most probably prevents a translocation, and therefore, only an initial binding of D-glucose to SGLT1 should be observed. It is noteworthy that the *p*-vinylsulfonylbenzoyl group is closely similar in size to the aglucone phloretin that is attached to the glycoside phlorizin which is not translocated by SGLT1. In this study, we observed distinct recognition events between the D-glucose-coupled cantilever and the living G6D3 cells. This interaction was Na^+-dependent and could be inhibited by phlorizin. Furthermore, as reported previously (*22*), it was only observed in CHO cells overexpressing SGLT1, thereby verifying the specificity of the interaction with SGLT1. Moreover, the observed unbinding force (f_u) required to disrupt this interaction and the binding probabilities of ∼8−12% were the same as in the previous study (*22*).

Selectivity of SGLT1-Mediated Sugar Transport. In general, the data presented here provide further support to previous studies which have shown the important roles of the hydroxyl groups on C2, C3, C4, and C6 in sugar binding and translocation by SGLT1 (*18*, *32*−*39*).

Substrate transport by SGLT1 has been proposed to proceed in several steps along the translocation pathway, including conformational alterations of the carrier and substrate translocation (*3*, *42*−*45*). Studies on the kinetics and substrate specificity of several isoforms of SGLT1, for instance, rabbit SGLT1, human SGLT1, and rat SGLT1, have demonstrated that each isoform exhibits individual properties (*18*). In any case, at least two sites of interaction of the transporter with the sugars are hypothesized to exist, one initial binding site and another in the translocation pathway. However, the direct experimental proof and characterization of these sites are lacking thus far.

In this study, an AFM force spectroscopy approach was used as a method for probing the initial D-glucose binding

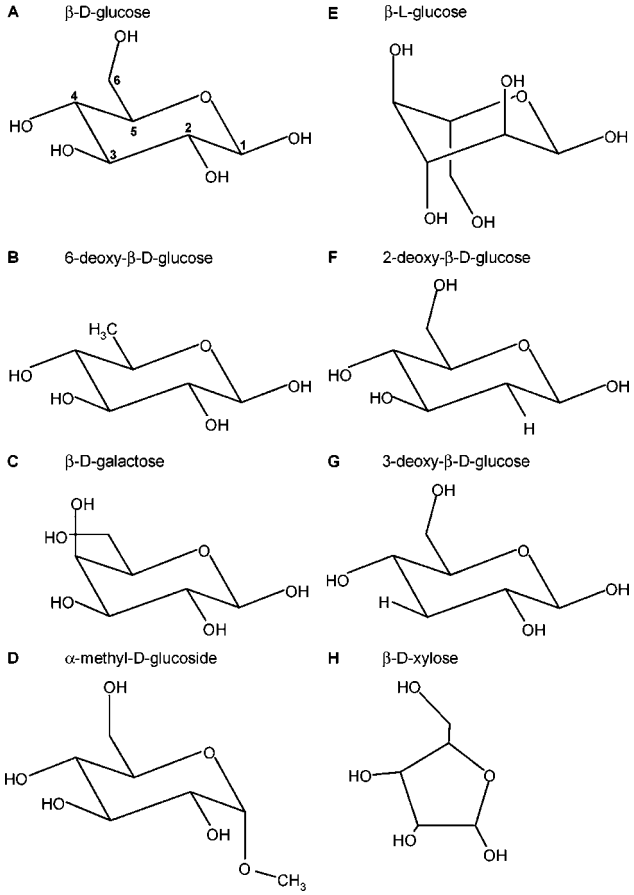

FIGURE 6: Chemical structure of the studied sugars. The ring form of *β*-D-glucose (A), 6-deoxy-*β*-D-glucose (B), *β*-D-galactose (C), α-methyl D-glucoside (D), *β*-L-glucose (E), 2-deoxy-*β*-D-glucose (F), 3-deoxy-*β*-D-glucose (G), and *β*-D-xylose (H) was generated with ISIS Draw 2.4.

properties of SGLT1. The changes in the probability of binding of the D-glucose-coupled AFM tip, reflecting the initial binding of D-glucose to SGLT1, were monitored before and after sugar injections. The probability of binding of the D-glucose tip was significantly reduced after application of free 6-deoxy-D-glucose, 2-deoxy-D-glucose, D-glucose, D-galactose, and α-methyl glucoside, whereas only a slight effect was observed in the presence of 3-deoxy-D-glucose, D-xylose, and L-glucose. The results indicate that the equatorial hydroxyl group on C3 (see the structure of sugars in Figure 6) is the most crucial feature to allow the initial interaction of sugars with rabbit SGLT1. D-galactose, a 4-epimer of D-glucose, has an axial configuration of the hydroxyl group on C4 which may impede the interaction of the C3 hydroxyl group with the carrier. These data are in accordance with the lower inhibitory potency of phloretin 2′-galactoside on sugar transport compared to that of the phloretin 2′-glucoside, phlorizin (*37*−*39*). Furthermore, it seems that a steric effect of a substituent on C1 plays a role in the accessibility of the sugar to SGLT1, which is evident from a slightly weaker inhibition by α-methyl glucoside (AMG).

It should be mentioned in this context that modification of the C3 hydroxyl group with a methyl group as in 3-*O*-methyl-D-glucose apparently still allows interaction with the initial docking site. 3-*O*-Methyl-D-glucose slightly inhibits phlorizin binding in rat kidney brush border membranes (*35*), and this sugar has been used as a model substance in studies of the cotransport of sodium and D-glucose. In those investigations, it exhibited characteristics similar to those of glucose but had a lower affinity (*46*).

In the study presented here, we further investigated the stereospecificity of sugar translocation by using competitive AMG uptake studies with the same sugars. These studies were necessary for obtaining a complete set of data for rabbit SGLT1 under the same conditions that were used in the AFM experiments. As expected, D-glucose and D-galactose exhibited the strongest inhibitory potency, followed by 6-deoxy-D-glucose. D-Xylose, 3-deoxy-D-glucose, and L-glucose exhibited a very weak or no inhibitory effect. This was anticipated from the AFM studies since the latter sugars also did not interact with the initial docking site. Most importantly, 2-deoxy-D-glucose exhibited an only slight inhibition of the AMG uptake, while it strongly inhibited the initial D-glucose binding in the AFM instrument (see above). These results suggest that the hydroxyl group on C2 is important for discriminating the sugars for translocation. A similar discrepancy between initial binding and translocation has been observed previously in rat kidney proximal tubule. 2-Deoxy-D-glucose was shown to inhibit binding of phlorizin to isolated brush border membrane vesicles, but no transepithelial transport was observed in microperfusion studies (*46*). This result raises the question of why 2-deoxy-D-glucose inhibits transport only slightly but strongly inhibits binding in the AFM and phlorizin binding studies. In a model where the two steps, binding and translocation, are assumed to be sequential, equal inhibition of binding and transport should be observed. Apparently in the presence of a large substituent at C1 such as the vinylsulfon group in the AFM studies or the two aromatic rings of phlorizin, the presence and positioning of the OH group at C2 seem to become irrelevant for the binding reaction; thus, both D-glucose and 2-deoxy-D-glucose act as inhibitors, based on the presence of the OH groups at C3, C4, and C6. This might be due either to conformational changes and steric hindrances at the glucose molecule itself or to similar events at the transporter. In the absence of a large substituent (and as a free sugar) like in the AMG uptake studies, rejection of 2-deoxy-D-glucose as a substrate probably occurs at the early binding site, and thus, the subsequent transport is not inhibited. Similar considerations seem not to apply to the OH group at C3 which is farther removed from the C1 position because 3-deoxy-D-glucose does not inhibit binding or transport to a significant extent.

When the results from the studies of the initial sugar binding and the competitive transport assays are combined, the following sequence of events in sugar recognition and selection for transport can be hypothesized. The sugars first reach a docking site which requires the presence of a hydroxyl group (or *O*-methyl group) at C3. The sugars fulfilling this requirement are then transferred to a second docking site which requires at C2 the presence of a hydroxyl group in the equatorial position, whereby mannose is also excluded which has a hydroxyl group in the axial position. Thereafter, the sugars can be translocated across the membrane. However, more detailed studies at the molecular level are needed to validate this assumption.

ACKNOWLEDGMENT

We thank Linda Wildling for helpful synthesis of the AFM cross-linkers. The generous help in the transport studies and cell culture from Kirsten Michel, Hendrike Schütz, Petra Glitz, and Christiane Pfaff is also gratefully acknowledged. Prof. Nateetip Krishnamra also provided generous support.

REFERENCES

1. Crane, R. K. (1977) The gradient hypothesis and other models of carrier-mediated active transport, *Rev. Physiol. Biochem. Pharmacol. 78*, 99−159.
2. Schultz, S. G., and Curran, P. F. (1970) Coupled transport of sodium and organic solutes, *Physiol. Rev. 50*, 637−718.
3. Wright, E. M. (2001) Renal Na^+-glucose cotransporters, *Am. J. Physiol. 280*, F10−F18.
4. Hediger, M. A., and Rhoads, D. B. (1994) Molecular physiology of sodium-glucose cotransporters, *Physiol. Rev. 74*, 993−1026.
5. Wright, E. M., and Turk, E. (2004) The sodium/glucose cotransport family SLC5, *Pfluegers Arch. 447*, 510−518.
6. Hediger, M. A., Coady, M. J., Ikeda, T. S., and Wright, E. M. (1987) Expression cloning and cDNA sequencing of the Na^+/glucose co-transporter, *Nature 330*, 379−381.
7. Wright, E. M., Turk, E., and Martin, M. G. (2002) Molecular basis for glucose-galactose malabsorption, *Cell Biochem. Biophys. 36*, 115−121.
8. Corpe, C., Sreenan, S., and Burant, C. (2001) Effects of type-2 diabetes and troglitazone on the expression patterns of small intestinal sugar transporters and PPAR-gamma in the Zucker diabetic fatty rat, *Digestion 63*, 116−123.
9. Tsujihara, K., Hongu, M., Saito, K., Kawanishi, H., Kuriyama, K., Matsumoto, M., Oku, A., Ueta, K., Tsuda, M., and Saito, A. (1999) Na^+-glucose cotransporter (SGLT) inhibitors as antidiabetic agents. 4. Synthesis and pharmacological properties of 4′-dehydroxyphlorizin derivatives substituted on the B ring, *J. Med. Chem. 42*, 5311−5324.
10. Lin, J., Kormanec, J., Homerova, D., and Kinne, R. K. (1999) Probing transmembrane topology of the high-affinity sodium/glucose cotransporter (SGLT1) with histidine-tagged mutants, *J. Membr. Biol. 170*, 243−252.
11. Turk, E., Kerner, C. J., Lostao, M. P., and Wright, E. M. (1996) Membrane topology of the human Na^+/glucose cotransporter SGLT1, *J. Biol. Chem. 271*, 1925−1934.
12. Turk, E., and Wright, E. M. (1997) Membrane topology motifs in the SGLT cotransporter family, *J. Membr. Biol. 159*, 1−20.
13. Panayotova-Heiermann, M., Eskandari, S., Turk, E., Zampighi, G. A., and Wright, E. M. (1997) Five transmembrane helices form the sugar pathway through the Na^+/glucose cotransporter, *J. Biol. Chem. 272*, 20324−20327.
14. Panayotova-Heiermann, M., Loo, D. D., Kong, C. T., Lever, J. E., and Wright, E. M. (1996) Sugar binding to Na^+/glucose cotransporters is determined by the carboxyl-terminal half of the protein, *J. Biol. Chem. 271*, 10029−10034.
15. Vayro, S., Lo, B., and Silverman, M. (1998) Functional studies of the rabbit intestinal Na^+/glucose carrier (SGLT1) expressed in COS-7 cells: Evaluation of the mutant A166C indicates this region is important for Na^+-activation of the carrier, *Biochem. J. 332* (Part 1), 119−125.
16. Nagata, K., and Hata, Y. (2006) Substrate specificity of a chimera made from *Xenopus* SGLT1-like protein and rabbit SGLT1, *Biochim. Biophys. Acta 1758*, 747−754.
17. Diez-Sampedro, A., Wright, E. M., and Hirayama, B. A. (2001) Residue 457 controls sugar binding and transport in the Na^+/glucose cotransporter, *J. Biol. Chem. 276*, 49188−49194.
18. Hirayama, B. A., Lostao, M. P., Panayotova-Heiermann, M., Loo, D. D., Turk, E., and Wright, E. M. (1996) Kinetic and specificity differences between rat, human, and rabbit Na^+-glucose cotransporters (SGLT-1), *Am. J. Physiol. 270*, G919−G926.
19. Kanai, Y., Lee, W. S., You, G., Brown, D., and Hediger, M. A. (1994) The human kidney low affinity Na^+/glucose cotransporter SGLT2. Delineation of the major renal reabsorptive mechanism for D-glucose, *J. Clin. Invest. 93*, 397−404.
20. You, G., Lee, W. S., Barros, E. J., Kanai, Y., Huo, T. L., Khawaja, S., Wells, R. G., Nigam, S. K., and Hediger, M. A. (1995) Molecular characteristics of Na^+-coupled glucose transporters in adult and embryonic rat kidney, *J. Biol. Chem. 270*, 29365−29371.
21. Binnig, G., Quate, C. F., and Gerber, C. (1986) Atomic force microscope, *Phys. Rev. Lett. 56*, 930−933.
22. Puntheeranurak, T., Wildling, L., Gruber, H. J., Kinne, R. K., and Hinterdorfer, P. (2006) Ligands on the string: single-molecule AFM studies on the interaction of antibodies and substrates with the Na^+-glucose co-transporter SGLT1 in living cells, *J. Cell Sci. 119*, 2960−2967.
23. Hinterdorfer, P., Baumgartner, W., Gruber, H. J., Schilcher, K., and Schindler, H. (1996) Detection and localization of individual antibody-antigen recognition events by atomic force microscopy, *Proc. Natl. Acad. Sci. U.S.A. 93*, 3477−3481.
24. Pfister, G., Stroh, C. M., Perschinka, H., Kind, M., Knoflach, M., Hinterdorfer, P., and Wick, G. (2005) Detection of HSP60 on the membrane surface of stressed human endothelial cells by atomic force and confocal microscopy, *J. Cell Sci. 118*, 1587−1594.
25. Wielert-Badt, S., Hinterdorfer, P., Gruber, H. J., Lin, J. T., Badt, D., Wimmer, B., Schindler, H., and Kinne, R. K. (2002) Single molecule recognition of protein binding epitopes in brush border membranes by force microscopy, *Biophys. J. 82*, 2767−2774.
26. Lee, G. U., Chrisey, L. A., and Colton, R. J. (1994) Direct measurement of the forces between complementary strands of DNA, *Science 266*, 771−773.
27. Lin, J. T., Kormanec, J., Wehner, F., Wielert-Badt, S., and Kinne, R. K. (1998) High-level expression of Na^+/D-glucose cotransporter (SGLT1) in a stably transfected Chinese hamster ovary cell line, *Biochim. Biophys. Acta 1373*, 309−320.
28. Castaneda, F., and Kinne, R. K. (2005) A 96-well automated method to study inhibitors of human sodium-dependent D-glucose transport, *Mol. Cell. Biochem. 280*, 91−98.
29. Butt, H.-J., and Jaschke, M. (1995) Calculation of thermal noise in atomic force microscopy, *Nanotechnology 6*, 1−7.
30. Hutter, J. L., and Bechhoefer, J. (1993) Calibration of atomic-force microscope tips, *Rev. Sci. Instrum. 64*, 1868−1873.
31. Baumgartner, W., Hinterdorfer, P., and Schindler, H. (2000) Data analysis of interaction forces measured with the atomic force microscope, *Ultramicroscopy 82*, 85−95.
32. Freire, C. A., Kinne-Saffran, E., Beyenbach, K. W., and Kinne, R. K. (1995) Na-D-glucose cotransport in renal brush-border membrane vesicles of an early teleost (*Oncorhynchus mykiss*), *Am. J. Physiol. 269*, R592−R602.
33. Kipp, H., Kinne-Saffran, E., Bevan, C., and Kinne, R. K. (1997) Characteristics of renal Na^+-D-glucose cotransport in the skate (*Raja erinacea*) and shark (*Squalus acanthias*), *Am. J. Physiol. 273*, R134−R142.
34. Wielert-Badt, S., Lin, J. T., Lorenz, M., Fritz, S., and Kinne, R. K. (2000) Probing the conformation of the sugar transport inhibitor phlorizin by 2D-NMR, molecular dynamics studies, and pharmacophore analysis, *J. Med. Chem. 43*, 1692−1698.
35. Glossmann, H., and Neville, D. M., Jr. (1972) Phlorizin receptors in isolated kidney brush border membranes, *J. Biol. Chem. 247*, 7779−7789.
36. Panayotova-Heiermann, M., Loo, D. D., and Wright, E. M. (1995) Kinetics of steady-state currents and charge movements associated with the rat Na^+/glucose cotransporter, *J. Biol. Chem. 270*, 27099−27105.
37. Diedrich, D. F. (1961) Comparison of effects of phlorizin and phloretin 2′-galactoside on the renal tubular reabsorption of glucose in dog, *Biochim. Biophys. Acta 47*, 618−620.
38. Diedrich, D. F. (1963) The comparative effects of some phlorizin analogs on the renal reabsorption of glucose, *Biochim. Biophys. Acta 71*, 688−700.
39. Diedrich, D. F. (1965) In vitro evaluation of relative inhibitory potency of phlorizin and its congeners, *Am. J. Physiol. 209*, 621−626.
40. Morpurgo, M., Veronese, F. M., Kachensky, D., and Harris, J. M. (1996) Preparation of characterization of poly(ethylene glycol) vinyl sulfone, *Bioconjugate Chem. 7*, 363−368.

41. Hinterdorfer, P., and Dufrene, Y. F. (2006) Detection and localization of single molecular recognition events using atomic force microscopy, *Nat. Methods 3*, 347−355.
42. Hirayama, B. A., Loo, D. D., and Wright, E. M. (1997) Cation effects on protein conformation and transport in the Na^+/glucose cotransporter, *J. Biol. Chem. 272*, 2110−2115.
43. Loo, D. D., Hirayama, B. A., Gallardo, E. M., Lam, J. T., Turk, E., and Wright, E. M. (1998) Conformational changes couple Na^+ and glucose transport, *Proc. Natl. Acad. Sci. U.S.A. 95*, 7789−7794.
44. Meinild, A. K., Hirayama, B. A., Wright, E. M., and Loo, D. D. (2002) Fluorescence studies of ligand-induced conformational changes of the Na^+/glucose cotransporter, *Biochemistry 41*, 1250−1258.
45. Loo, D. D., Hirayama, B. A., Cha, A., Bezanilla, F., and Wright, E. M. (2005) Perturbation analysis of the voltage-sensitive conformational changes of the Na^+/glucose cotransporter, *J. Gen. Physiol. 125*, 13−36.
46. Kinne, R. K. (1976) Properties of the glucose transport system in the renal brush border membrane, *Curr. Top. Membr. Transp. 8*, 209−267.

BI061917Z